Hindawi Publishing Corporation
International Journal of Photoenergy
Volume 2012, Article ID 859294, 12 pages
doi:10.1155/2012/859294

Research Article

Photoetching of Immobilized TiO_2-ENR_{50}-PVC Composite for Improved Photocatalytic Activity

M. A. Nawi, Y. S. Ngoh, and S. M. Zain

School of Chemical Sciences, Universiti Sains Malaysia, Minden 11800, Malaysia

Correspondence should be addressed to M. A. Nawi, masri@usm.my

Received 23 February 2012; Accepted 26 March 2012

Academic Editor: Stéphane Jobic

Commercially acquired TiO_2 photocatalyst (99% anatase) powder was mixed with epoxidized natural rubber-50 (ENR_{50})/polyvinyl chloride (PVC) blend by ultrasonication and immobilized onto glass plates as TiO_2-ENR_{50}-PVC composite via a dip-coating method. Photoetching of the immobilized TiO_2-ENR_{50}-PVC composite was investigated under the irradiation of a 45 W compact fluorescent lamp and characterized by chemical oxygen demand (COD) analysis, scanning electron microscopy-energy dispersive X-ray (SEM-EDX) spectrometry, thermogravimetry analysis (TGA), and fourier transform infrared (FTIR) spectroscopy. The BET surface area of the photoetched TiO_2 composite was observed to be larger than the original TiO_2 powder due to the systematic removal of ENR_{50} while PVC was retained within the composite. It also exhibited better photocatalytic efficiency than the TiO_2 powder in a slurry mode and was highly reproducible and reusable. More than 98% of MB removal was consistently achieved for 10 repeated runs of the photo-etched photocatalyst system. About 93% of the 20 mg L^{-1} MB was mineralized over a period of 480 min. The presence of SO_4^{2-}, NO_3^-, and Cl^- anions was detected in the mineralized solution where the solution pH was reduced from 7 to 4.

1. Introduction

Semiconductor TiO_2 has been broadly studied as a heterogeneous photocatalyst for the decomposition of hazardous compounds in water effluents, including organic dyes [1–3]. TiO_2 is highly effective for producing oxidizing species, specifically $HO^\bullet$ radicals, which possess significant oxidation potential. Other advantages of TiO_2 include its biological and chemical stability, nontoxicity, low cost, and availability [3]. However, as the use of this catalyst for photocatalytic reactions is usually carried out in slurry modes, the need for posttreatment or filtration step makes its practical applications tedious and costly. Therefore, effective immobilization technique of the catalyst for industrial scale application is highly needed. However, immobilization of the catalyst onto solid supports poses its own intrinsic problems. Due to the fixed surface area, the photocatalytic activity of the immobilized catalyst is often significantly reduced [4–6]. Some other inherent problems created by immobilization of the photocatalyst are potential loss of TiO_2 and decreased adsorption of organic substances on the TiO_2 surface [7]. Thus, the major challenge in industrializing this technology seems to lay in the effective immobilization of photocatalyst on solid support without decreasing its photocatalytic activity.

The use of rubber-related polymer for the immobilization of TiO_2 powder has been explored by a number of researchers. Jin et al. [8] formed TiO_2 layer on a natural rubber substrate via liquid phase deposition while Sriwong et al. [9] incorporated TiO_2 powder into rubber sheet in order to immobilize TiO_2 powder. As for Silva et al. [10], they compounded silicone rubbers with TiO_2 for the purpose of immobilizing TiO_2. While most of these works reported good photocatalytic activities in removing their respective pollutants, no efforts have been made to monitor what happened to the rubber additive during irradiation of their photocatalytic systems. In other works, Nawi et al. [11, 12] had previously reported the use of ENR_{50} and ENR_{50}/phenol formaldehyde (PF) blend, respectively, for the immobilization of TiO_2 powder over aluminum using electrophoretic deposition and dip-coating method on glass plates for the removal of phenol. As reported by Nawi et al. [12], the ENR additive was highly degradable and could be

photocatalytically photoetched out and served as the precursor for the formation of pores and also once completely removed from the immobilized photocatalyst could increase the surface area, pore volume of the immobilized P-25 TiO_2 particles.

Polymer blends have become a subject of interest in the field of polymeric materials since their individual properties can be modified to obtain desired new properties. Polymer blending is known to improve mechanical, environmental, and rheological properties of the polymers. One widely studied polymer blend is epoxidized natural rubber-50 (ENR_{50})/poly(vinyl) chloride (PVC), which is found to form miscible blends at any compositions ratio [13]. The excellent miscibility between ENR_{50} and PVC is believed to be induced by the highly polar epoxide groups within the ENR_{50} molecules [14]. PVC is also anticipated to provide high tensile strength and good chemical resistance while ENR can act as a plasticizer for PVC [15]. In fact, the mechanical properties of ENR_{50}/PVC have been widely studied and reported in the literatures [13, 16].

The main objective of this work was to prepare a highly reusable immobilized TiO_2-ENR_{50}-PVC composite having comparable or better photocatalytic activity than the catalyst powder applied in a slurry mode. In order to achieve this objective, the surface area of the immobilized catalyst composite would be improved via photoetching of the polymer additive under light irradiation. The photo-etched catalyst composite would also be systematically characterized in order to understand the surface transformation process that occurred during the etching process. We also evaluated the photomineralization capability of the prepared immobilized TiO_2 composite by using methylene blue (MB) as the model pollutant. The reusability and reproducibility of the TiO_2 composite in the degradation of MB were also tested. Therefore, this method was developed as a new approach in producing immobilized TiO_2 photocatalyst with comparable or better photocatalytic efficiency than the slurry mode but with long-term reusability and without the cumbersome filtration step of the treated water.

2. Materials and Methods

2.1. Chemicals. All chemicals were of analytical grades and used without further purification. Titanium (IV) oxide (TiO_2) (99% anatase) was purchased from Sigma Aldrich. Epoxidized natural rubber (50% epoxidation) (ENR_{50}) was from Guthrie Group Limited. The 12% (w/w) ENR_{50} solution was prepared by refluxing 25.80 ± 0.05 g solid ENR_{50} in 250 mL toluene (from BDH AnalaR) at 88–90°C over a period of 80 h until it was completely dissolved. Poly (vinyl) chloride (PVC) powder was purchased from Petrochemicals (Malaysia) Sdn. Bhd. The *K* value of the PVC powder was 67. Acetone was obtained from Systerm and dichloromethane was a product from R&M Chemicals. Methylene blue (MB) (~98%, Colour Index Number: 52015, chemical formula: $C_{16}H_{18}ClN_3S \cdot 2H_2O$, λ_{max}: 661 nm) was purchased from Unilab, Ajax Chemicals. The 1000 mg L^{-1} MB stock solution was prepared by dissolving 1.00 g MB powder in 1 L ultrapure water. For chemical oxygen demand (COD) analysis, digester and COD reagent solutions were purchased from HACH.

2.2. Preparation of Immobilized TiO_2-ENR_{50}-PVC Composite

2.2.1. Preparation of TiO_2-ENR_{50}-PVC Dip-Coating Formulation. The TiO_2-ENR_{50}-PVC dip-coating formulation was prepared by dissolving 0.80 g of PVC powder in 35 mL of dichloromethane and sonicated using ultrasonic cleaner (Crest Ultrasonics, 50 kHz) for 1 h. Then, 2 g of 12% (w/w) ENR_{50} solution and 65 mL of acetone were added before adding 12 g of TiO_2 powder. The mixture was then homogenized via ultrasonication for 5 h at 30–40°C. The prepared formulation was kept in an amber bottle to avoid the exposure of the formulation to light.

2.2.2. Deposition of TiO_2-ENR_{50}-PVC Composite onto Glass Plates. For coating the TiO_2-ENR_{50}-PVC composite onto the glass plates, the formulation was poured into a custom made coating cell. The dip-coating process was then done by immersing a preweighed cleaned glass plate with the dimension of 4.0 cm × 7.5 cm into the dip-coating formulation with uniform pulling rates. Before weighing the coated glass plate, it was left to dry in an oven at 50°C for 5 minutes in order to allow the evaporation of the solvents. The process of coating-drying-weighing was done repeatedly until the desired amount of TiO_2-ENR_{50}-PVC composite was deposited onto the glass plate. The TiO_2-ENR_{50}-PVC composite loading used throughout this work was 1.00 mg cm^{-2}.

The optimum composition of the dip-coating formulation (i.e., the amount of ENR_{50} solution, PVC powder and TiO_2 powder) was obtained upon systematically varying each component of the formulation for optimum photocatalytic activity and acceptable adhesion of the photocatalyst composite onto the glass plates. The adhesion test of the series of immobilized TiO_2 composites with different ratio of ENR_{50} and PVC was carried out using a sonication test. In this test, the respective glass plates coated with TiO_2-ENR_{50}-PVC composite were first immersed in a beaker filled with ultrapure water and then were subjected to an interval of 5 s sonication in an ultrasonic cleaner until 30 s. After each successive intermittent sonication, the remaining coating that still adhered onto the glass plate was dried and weighed. The glass plate with the largest remaining TiO_2-ENR_{50}-PVC composite coating would be considered as having the highest degree of adhesion. The adhesion of the TiO_2-ENR_{50}-PVC composite with different amounts of ENR_{50} and PVC was then compared against the reference plate, which was made of TiO_2-ENR_{50} or TiO_2-PVC in order to find out their relative strength. The relative strength values were obtained by manipulating the following equation (1):

$$\frac{\mathrm{SP} - \mathrm{RP}}{\mathrm{CP_i}} \times 100 = \text{relative strength (\%)}, \quad (1)$$

where SP is the remaining weight of the TiO_2-ENR_{50}-PVC composite after 30 s of sonication. RP is the reference plate that could be either TiO_2-ENR_{50} or TiO_2-PVC composite also after 30 s of sonication, respectively, while CP_i is

the initial weight of control plates that could be TiO_2-ENR_{50}-PVC, TiO_2-ENR_{50}, or TiO_2-PVC plate where each of them was controlled to have a similar weight value.

2.3. Photo-Etching of the TiO_2-ENR_{50}-PVC Composite and Its Characterizations. Chemical oxygen demand (COD) test was carried out to detect the photodegradation of ENR_{50}/PVC within the TiO_2 composite. In this test, the glass plate with immobilized TiO_2 composite was immersed in ultra pure water in a glass cell and irradiated under a 45 W household fluorescent lamp (see Figure 1 for the reactor design). The COD analyses of the ultrapure water samples after predefined irradiation times were determined by refluxing the treated solution in a COD digester (model 45600-02, HACH). Meanwhile, the changes in the morphology of the photo-etched TiO_2 composite were observed using a scanning electron microscope (SEM, model LEO SUPRA 50 VP Field Emission) while energy dispersive X-ray (EDX) and CHN analyzer were used to determine the element composition of the photo-etched TiO_2 composites.

The photocatalytic degradation of the polymer blends within the TiO_2 composite was further investigated by subjecting the non-etched and the photo-etched TiO_2 composite to a thermogravimetry analyzer (TGA, STAR^e model Mettler Toledo) in order to detect the remaining polymer content of the composites before and after irradiation. For comparison purposes, ENR_{50} and PVC were also, respectively, analyzed with TGA. The TGA analysis was performed in N_2 atmosphere at a heating rate of 10°C min^{-1} from 30°C to 800°C. Fourier transform infrared (FTIR, Perkin Elmer FTIR System Model 2000) spectrometry was also carried out from 400–4000 cm^{-1} to see the alteration of the functional groups of the TiO_2 composites after subsequent irradiation. The KBr pellets for IR analysis were prepared using well-dried samples by leaving the samples in an oven at 60°C for 5 days.

2.4. Photocatalytic Degradation of MB. Photocatalytic activity of the photoetched immobilized TiO_2-ENR_{50}-PVC composite was investigated using MB solution as the model pollutant and by employing the reactor shown in Figure 1. A 45 W compact fluorescent lamp with a UV leakage irradiance of 4.35 Wm^{-2} was placed in contact with the outer surface of the (5.0 cm × 8.0 cm × 1.0 cm) glass reactor cell containing 20 mL of 12 mg L^{-1} MB solution. The UV leakage irradiance of the light source was measured using a Solar light co. PMA 2100 radiometer connected with UV-A and UV-B broadband detector (PMA 2107). The photo-etched immobilized TiO_2-ENR_{50}-PVC composite was placed uprightly inside the photoreactor cell and was exposed directly to the light source. The MB solution was bubbled with air supplied by an aquarium pump and was maintained at a flow rate of 40 mL min^{-1} throughout the photocatalytic treatment using a Gilmont direct reading flow meter.

The photocatalytic efficiency of the photo-etched immobilized TiO_2-ENR_{50}-PVC composite was assessed by monitoring the degradation of the MB solution at every interval of 15 min for 90 min using the UV-Vis spectrophotometer (HACH model DR2000) at the wavelength of 661 nm.

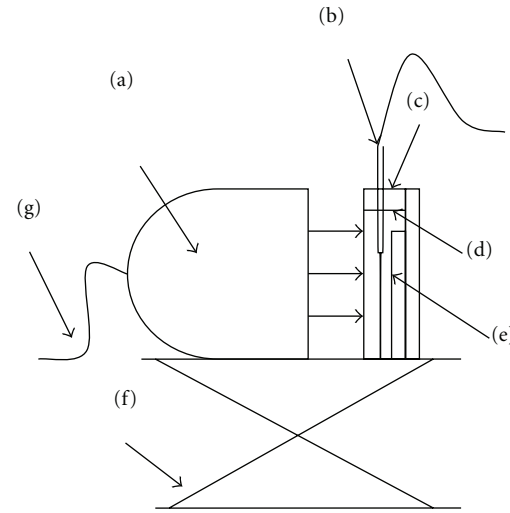

Figure 1: The experimental setup for photocatalytic studies consists of (a) 45 W fluorescent lamp, (b) aeration supply from aquarium pump, (c) custom made glass cell, (d) model pollutant, (e) immobilized TiO_2 composite, (f) scissor jack, and (g) power supply.

Adsorption study and photolysis experiment were done in a similar manner except that the cell reactor was placed in a box and without the presence of the catalyst. For the purpose of performance comparisons, photocatalytic evaluation involving TiO_2 slurry mode was carried out using a similar experimental set-up except that the TiO_2 powder was employed and the degraded MB solution was filtered using 0.20 μm nylon filter to separate the catalyst particles at every interval of 15 minutes before its absorbance reading was taken.

For the reproducibility and reusability study of the photo-etched immobilized TiO_2-ENR_{50}-PVC composite, the immobilized photocatalyst composite was subjected for 10 repeated cycles of MB degradation where each cycle took 90 min. The percentage of MB that remained at each interval was calculated according to the following equation (2):

$$\text{MB remained (\%)} = \frac{\text{Co} - \text{Ct}}{\text{Co}} * 100, \tag{2}$$

where Co (mg L^{-1}) and Ct (mg L^{-1}) were concentrations of MB before and after treatment at time t, respectively. The degradation of MB by the photo-etched TiO_2-ENR_{50}-PVC composite was best fitted by pseudo-first-order kinetics. The related kinetic model is shown in:

$$\ln\left(\frac{\text{Co}}{\text{Ct}}\right) = kt, \tag{3}$$

where Co and Ct are the initial MB concentration and the concentration at time t (min), respectively, t is the irradiation time (min), and k is the pseudo-first-order rate constant (min^{-1}).

2.5. Photocatalytic Mineralization of MB. The photocatalytic mineralization of 20 mg L^{-1} MB by the photo-etched immobilized TiO_2-ENR_{50}-PVC composite was studied over

a period of 8 h and the COD, SO_4^{2-}, NO_3^-, and Cl^- concentrations as well as the change of solution pH in the treated MB were noted hourly. The COD analyses of the MB solution were carried as elaborated in Section 2.3 whereby the COD digester and water samples were refluxed. The photomineralization efficiency of the photo-etched immobilized TiO_2-ENR_{50}-PVC composite was calculated according to the following equation:

$$\text{COD remained (\%)} = \frac{\text{COD}_\text{i} - \text{COD}_\text{f}}{\text{COD}_\text{i}} * 100, \quad (4)$$

where COD_i (mg L^{-1}) and COD_f (mg L^{-1}) were concentrations of COD in solution before and after hourly photo-mineralization. The generated inorganic anions were detected using ion chromatograph (IC, Metrohm model 792 Basic IC). A pH meter (Orion) was used to monitor the changes in pH of the treated MB solutions.

3. Results and Discussion

3.1. TiO_2-ENR_{50}-PVC Dip-Coating Formulation. Results from the optimization study (see Table 1) indicated that although the degree of adhesion of the composite onto the support increased proportionately with the amount of either polymer, the trend showed that addition of beyond 0.8 g PVC and 2 g ENR_{50} reduced its photocatalytic efficiency. As will be discussed later in Section 3.3, this was due to the extensive coverage of the polymer upon the surface of the photocatalyst which inadvertently lowered its photocatalytic activity. Apparently 0.8 g PVC and 2 g of 12% ENR_{50} solution were the optimum polymeric loadings since this blend provided the optimum pseudo-first-order rate constant values for the degradation of MB and acceptable relative adhesion strength. As 2 g of ENR_{50} solution was equivalent to 0.24 ± 0.05 g solid ENR_{50}, the ratio of the optimum mixture of TiO_2, PVC, and ENR_{50} in the dip-coating formulation in term of solid weight was 50 : 3 : 1.

3.2. Photo-Etching of the Immobilized TiO_2-ENR_{50}-PVC Composite. Many polymers are not resistant towards light and oxidizing environment. In the presence of light, they tend to undergo photolysis and degrade. Furthermore, it has been reported that TiO_2 particles have significant photocatalytic effects on polymers such as polyethylene and polyvinyl chloride due to the generation of highly oxidizing species under UV light [17, 18]. Therefore, ENR_{50}/PVC polymers can be systematically photoetched out to modify the surface of the immobilized catalyst. This etching process was expected to enhance the surface area of the immobilized catalyst composite. The etching process was evaluated by irradiating the immobilized composite in ultrapure water for a predefined time and the subsequent COD concentration of the water was monitored. The detected COD values in the treated water indicated that the organic polymers were degraded to produce dissolved organic matter (DOM). Figure 2 shows that upon one hour of irradiation of the immobilized TiO_2/ENR_{50}/PVC composite, the COD concentration of the water sample was found to be 73 ± 3 mg L^{-1} and it subsequently decreased over the evaluated period until it became essentially zero. As the polymer blend was subsequently photo-etched out, the organic residual within the composite decreased and since the exposed water was changed every hour, its COD concentration continued to decrease until negligible leaching of DOM was observed beyond the 8th hour of irradiation. It can be assumed from Figure 2 that the etching process was completed in the 9th hour of irradiation.

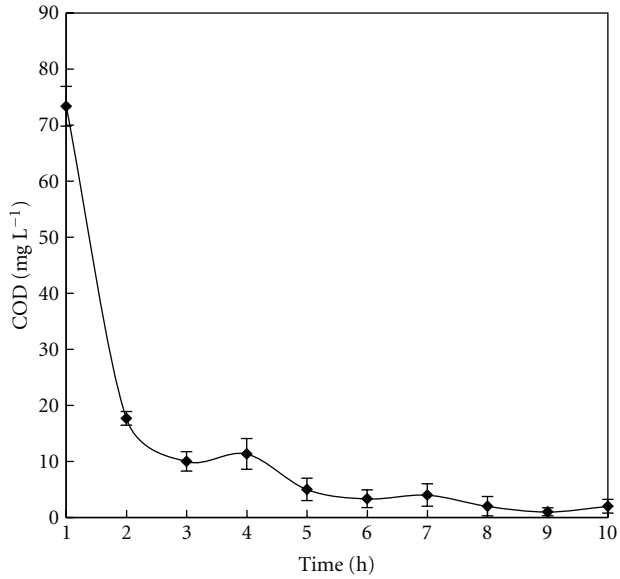

Figure 2: COD concentration of water sample with photo-etched TiO_2-ENR_{50}-PVC composite over the span of 10 hours.

3.3. Characterization of the Photo-Etched Immobilized TiO_2-ENR_{50}-PVC Composite. The surface morphology of TiO_2 powder as shown by the SEM micrograph in Figure 3(a) was made up of evenly distributed particles with no apparent signs of agglomerations. The particles were held closely to one another, giving its surface a smooth-like texture. The SEM micrographs of the TiO_2-ENR_{50}-PVC composites before and after etching process are shown in Figures 3(b) and 3(c) while their related elemental analyses results are provided in Table 2, respectively. The micrograph of the non-etched TiO_2-ENR_{50}-PVC composite showed in Figure 3(b) exhibits extensive aggregations of TiO_2 particles with irregular emergence of pores with visible depths. The catalyst particles were heavily agglomerated and are seen to be covered by whitish layers which are believed to be the polymer blends. As seen in Figure 3(c), the photo-etched TiO_2-ENR_{50}-PVC composite via irradiation for 9 h clearly shows the elimination of the sticky whitish layers that enveloped the TiO_2 particles even though aggregations of TiO_2 particles and porous depths are still observed.

The EDX elemental analyses results of the composites in Table 2 show that the amount of carbon dropped drastically from 9.14 ± 0.87 to 1.50 ± 0.18% after the photo-etching process. The amount of Cl element detected within the photo-etched composite also decreased significantly. These

Table 1: (a) Pseudo-first-order rate constants for the adsorption and photocatalytic degradation of 12 mg L^{-1} MB in aqueous solution by TiO_2-5 g ENR_{50}-PVC formulations with different amount of PVC and (b) TiO_2-ENR_{50}-0.8 g PVC with different amount of ENR_{50} as well as their respective relative adhesion strength upon the glass plates. TiO_2 powder was maintained at 12 g.

PVC (g)	ENR sol. (g)	Pseudo-first-order rate constants (min^{-1})		Relative strength (%)
		Adsorption	Photocatalysis	
(a)				
0.0	5	0.0049	0.0180	0.00
0.1	5	0.0047	0.0165	—
0.2	5	0.0048	0.0176	5.97
0.3	5	0.0050	0.0180	—
0.4	5	0.0054	0.0184	12.62
0.5	5	0.0055	0.0186	—
0.6	5	0.0056	0.0189	15.75
0.7	5	0.0064	0.0198	—
0.8	5	0.0068	0.0205	29.86
0.9	5	0.0034	0.0172	—
1.0	5	0.0028	0.0094	20.50
(b)				
0.8	0.0	0.0045	0.0207	0.00
0.8	1.0	0.0048	0.0208	15.21
0.8	2.0	0.0049	0.0276	18.21
0.8	3.0	0.0045	0.0189	22.54
0.8	4.0	0.0052	0.0185	25.26
0.8	5.0	0.0068	0.0205	29.86

Table 2: (a) EDX and (b) CHN analyses of the nonetched TiO_2-ENR_{50}-PVC composite and the photoetched TiO_2-ENR_{50}-PVC composites.

Sample	Weight (%)				
	Carbon	Hydrogen	Oxygen	Titanium	Chloride
(a) EDX					
TiO_2 composite	9.14 ± 0.87	—	40.20 ± 2.10	49.93 ± 3.54	1.04 ± 0.14
Etched TiO_2 composite	1.50 ± 0.18	—	40.06 ± 0.60	58.20 ± 0.74	0.25 ± 0.04
(b) CHN					
TiO_2 composite	4.61	0.51			
Etched 3 h	3.22	0.09			
Etched 6 h	3.15	0.15			
Etched 9 h	1.39	0.01			
Etched 10 h	1.20	0.05			

results further confirmed that the ENR_{50}/PVC blends within the TiO_2 composite were degraded to a certain degree by the applied light source. These results support the COD analyses obtained earlier in Section 3.2. A detailed stepwise monitoring of the etching process of the immobilized TiO_2-ENR_{50}-PVC composite via CHN analysis is provided in (b) of Table 2. The value of C element decreased with time of irradiation indicating the continuous removal of the polymer blend. It can be inferred from here that the etching process was completed after 9 h of irradiation since the value of C element remained more or less constant beyond this time which was once again in good agreement with the previous EDX and COD analyses.

Figure 4 illustrates the TGA and DTG curves of ENR_{50}, PVC and TiO_2-ENR_{50}-PVC composites before and after photo-etching. The corresponding thermogravimetric data is provided in Supplementary Table 1 (in Supplementary Material available online at doi: 10.1155/2012/859294). The degradation of ENR_{50} shown in Figure 4(a) occurred in one stage with the maximum weight loss temperature (T_{max}) at 400°C. The weight loss was determined to be 98.56%. The degradation of ENR_{50} was initiated by the fragmentation of polyisoprene chains and the epoxy polar groups, producing volatile components such as isoprene and dipentene [14]. On the other hand, Figure 4(b) shows that the degradation of PVC occurred in two stages. The first stage occurred at

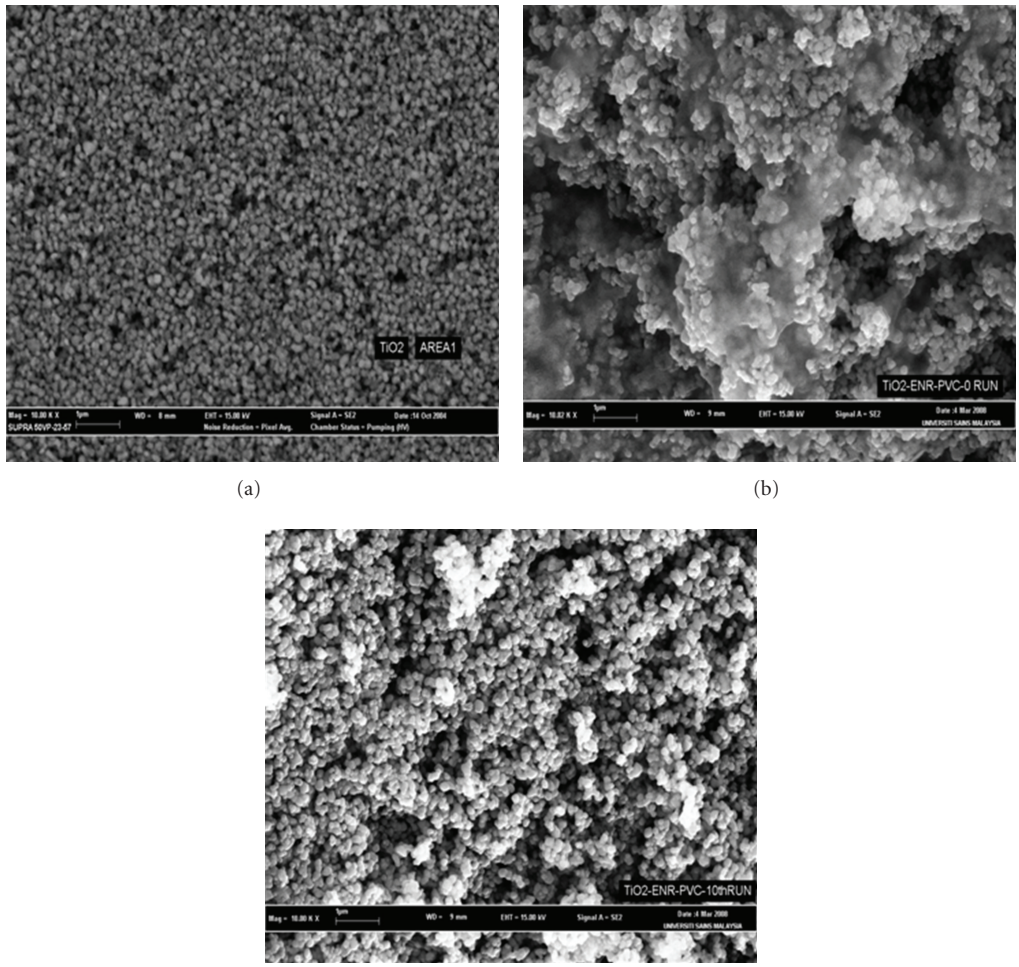

(a) (b)

(c)

Figure 3: SEM micrographs of (a) TiO_2 powder, (b) nonetched TiO_2-ENR_{50}-PVC composite, and (c) photo-etched TiO_2-ENR_{50}-PVC composite under 10,000 x magnification.

230–350°C with T_{max} at 300°C while the second stage of the PVC degradation happened at 380−500°C with T_{max} at 450°C.The first stage of the degradation process corresponds to the elimination of HCl molecules from the polyene chains whereas the second dominant stage refers to the degradation of the polyene structure, yielding volatile aromatic and aliphatic compounds from the conjugated sequences [19]. It was also observed from the DTG curve of PVC, that there was a shoulder peak after the first stage, indicating the pyrolysis of the HCl residuals of PVC [19]. This peak became more obvious in the DTG curve of the TiO_2-ENR_{50}-PVC composite shown in Figure 4(c) where three degradation stages of the composite were observed. The first and second degradation stage can be associated with the dehydrochlorination of PVC while the last degradation stage was due to the degradation of both the ENR_{50} and PVC. Nair et al. [19] observed two dominant degradation stages during the TGA analysis of polymer blend ENR_{50}/PVC where they attributed the first degradation stage to PVC and the second degradation stage to the decomposition of ENR_{50} and PVC. The TGA and DTG curves of the photo-etched TiO_2 composite are shown in Figure 4(d). It exhibits only one degradation stage with T_{max} at 300°C. This can be ascribed to the dehydrochlorination of the PVC. In short, after the etching process of the TiO_2 composite, it may be deduced that PVC is still predominantly present within the TiO_2 composites. This is in line with Table 2 whereby elemental C was detected even after 10 h of irradiation and this could be due to the presence of PVC within the composite as supported by the detection of Cl within the composite.

The FTIR spectra of TiO_2 powder, TiO_2-ENR_{50}, TiO_2-PVC, TiO_2-ENR_{50}-PVC composite and the photo-etched TiO_2-ENR_{50}-PVC composite are shown in Figures 5(a)–5(e), respectively. The presence of ENR_{50} and PVC within the TiO_2 composite were qualitatively identified by comparing the FT-IR spectra of TiO_2-ENR_{50} (Figure 5(b)) and TiO_2-PVC (Figure 5(c)) with TiO_2 powder (Figure 5(a)) and TiO_2-ENR_{50}-PVC composite (Figure 5(d)). The bands attributed to the presence of ENR_{50} in the composite are confirmed by the C–H stretching vibrations of the polymer main chains

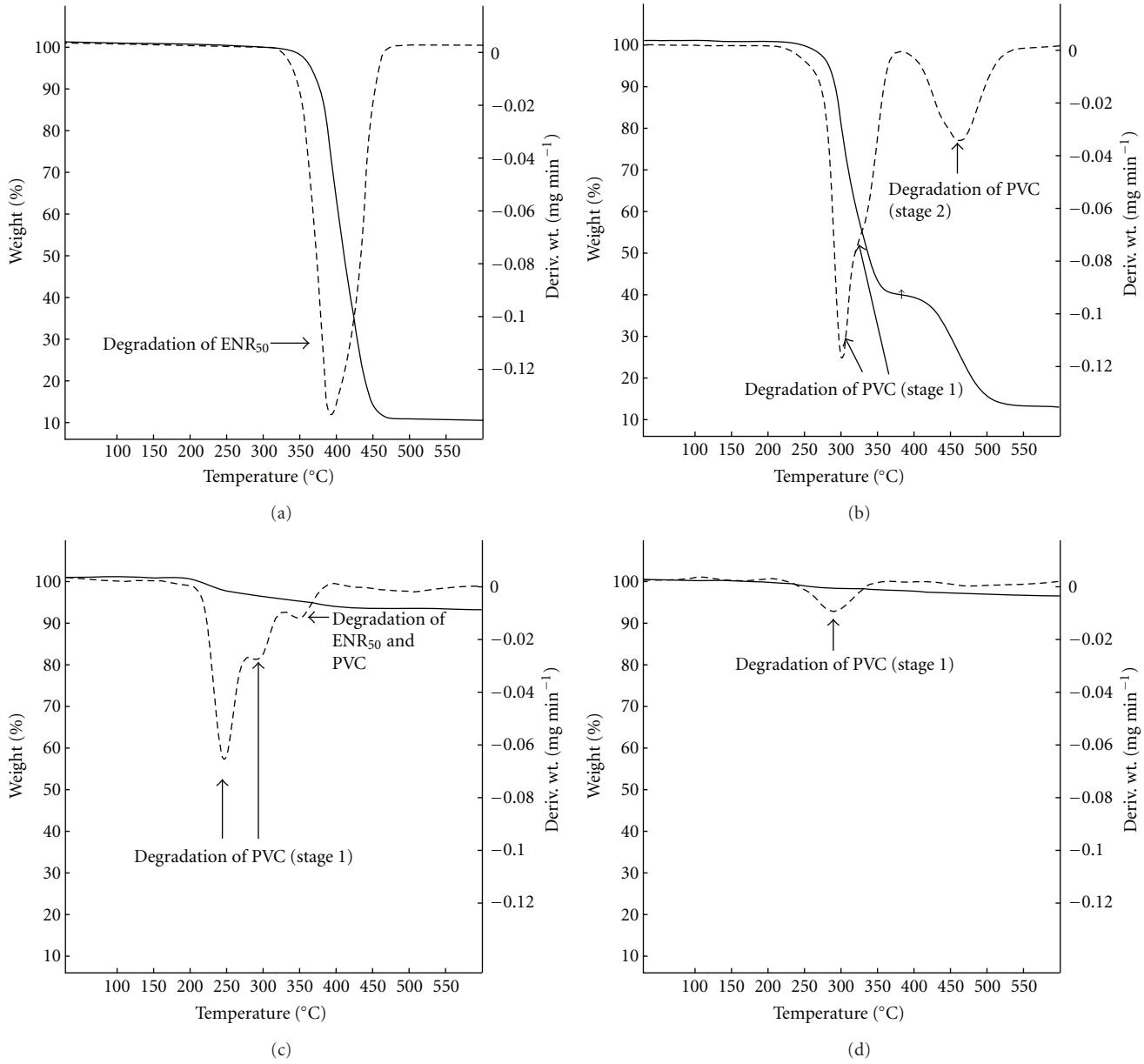

Figure 4: TGA and DTG curves of (a) ENR_{50}, (b) PVC, (c) non-etched TiO_2-ENR_{50}-PVC composite, and (d) photo-etched TiO_2-ENR_{50}-PVC composite.

$–CH_2–$ (asymmetric) and $–CH_3$, C–H bending vibrations and the O–H stretching of hydroxyl groups at peak 2937, 1378, and 3000–3500 cm^{-1}, respectively. Meanwhile, the absorption bands at 1330, and 1257 cm^{-1} show the deformation of $–CH_2–$ and CH rocking vibration of the CH_2Cl bonds only when PVC was included into the composite [14]. It can be concluded from Figure 5 that the spectrum of the TiO_2-ENR_{50}-PVC composite is a combined spectra of the TiO_2-ENR_{50} and TiO_2-PVC.

After irradiation for 10 h, the photo-etched TiO_2 composite produced the IR spectrum shown in Figure 5(e). It can be observed that the intensity of the absorption band at 2900 cm^{-1} region which represents the C–H stretching vibrations of the polymer $–CH_2–$ (asymmetric) and $–CH_3$ in ENR_{50} was reduced. The photoetching of ENR_{50} was also indicated by the absence of the C–H bending vibrations band at 1376 cm^{-1}. The photoetching of PVC in the irradiated immobilized TiO_2-ENR_{50}-PVC composite was also indicated by the reduction in the absorption band at 1331 and 1254 cm^{-1}, signifying the destruction of CH_2 deformation and CH_2Cl bonds, respectively. Figure 5(e) also shows the appearance of two new absorption bands at 1192 and 1151 cm^{-1}. These absorption bands may be attributed to the formation of aliphatic ether which suggests the cross-linking interactions between the two polymers. It has been reported that ENR_{50} and PVC are capable of forming self cross-linkable blends. Ratnam and Zaman [16] also observed the emergence of two absorption bands at 1100 cm^{-1} region

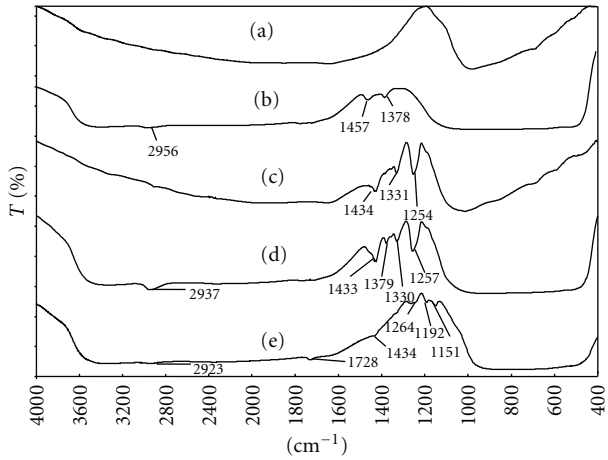

Figure 5: FTIR spectra of (a) TiO_2 powder, (b) TiO_2/ENR_{50}, (c) TiO_2/PVC, (d) non-etched TiO_2-ENR_{50}-PVC composite, and (e) photo-etched TiO_2-ENR_{50}-PVC composite.

when studying the effect of cross-linking agent on the properties of ENR_{50}/PVC. Thus, the exposure of the TiO_2-ENR_{50}-PVC composite to irradiation and oxidizing condition did not only induce the degradation of the polymers but also initiated the cross-linking of the polymers within the composite.

The photocatalytic degradation of the polymer blend within the composite occurred due to the presence of highly oxidizing radicals. As the TiO_2 particles of the composite are stimulated by UV irradiation from the light source, highly oxidizing radicals such as $O_2^{\bullet -}$, $HOO^{\bullet}$, and $HO^{\bullet}$ were generated (5). These active oxygen species then induced the degradation reactions by attacking the neighbouring polymer chains or by diffusing into the polymer matrix to form carbon-centered radicals. Their following reactions with the photogenerated oxidizing radicals lead to the production of oxidized species such as carbonyl intermediates [8, 17] and eventually to CO_2 and H_2O:

$$\begin{aligned} TiO_2 + h\nu &\longrightarrow TiO_2 * (e_{cb}^{-} + h_{vb}^{+}) \\ e_{cb}^{-} + O_2 &\longrightarrow O_2^{\bullet -} \\ O_2^{\bullet -} + H_2O &\longrightarrow HOO^{\bullet} + OH^{-} \\ 2HOO^{\bullet} &\longrightarrow H_2O_2 + O_2 \\ H_2O_2 + h\nu &\longrightarrow 2HO^{\bullet} \\ h_{vb}^{+} + H_2O &\longrightarrow HO^{\bullet} \end{aligned} \quad (5)$$

The nitrogen adsorption isotherms for the TiO_2 powder, TiO_2-ENR_{50}-PVC composite and the photo-etched TiO_2-ENR_{50}-PVC, composite are provided in Figure 6. As can be seen, the isotherms for all cases resemble type II based on the IUPAC system, which correlates with the nonporous solids. Their shape indicates that no significant differences in surface texture exist. However, isotherms for the photo-etched samples absorbed slightly more nitrogen at lower pressure than the TiO_2 powder which is due to the presence of larger

Table 3: Microstructures of TiO_2 powder, nonetched TiO_2-ENR_{50}-PVC composite, and photoetched TiO_2-ENR_{50}-PVC composite.

Samples	BET surface area ($m^2\ g^{-1}$)	Total pore volume ($cm^3\ g^{-1}$)	Average pore diameter (nm)
TiO_2 powder	10.17	0.0237	9.348
TiO_2 composite	5.44	0.0161	11.846
Etched TiO_2 composite	15.24	0.0244	6.418

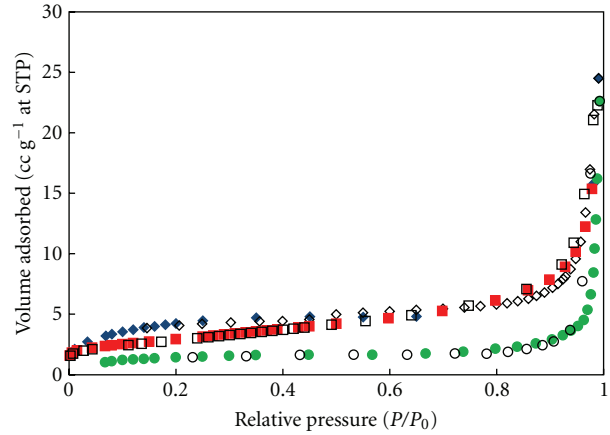

Figure 6: Nitrogen adsorption (coloured) and desorption (open) isotherm of TiO_2 powder (red square), non-etched TiO_2-ENR_{50}-PVC composite (green circle) and etched TiO_2-ENR_{50}-PVC composite (blue diamond).

pore volumes and surface area. It was also observed that the non-etched TiO_2-ENR_{50}-PVC composite adsorbed the least nitrogen indicating that its surface area was the lowest. The BET surface area, total pore volumes, and average pore diameters are listed in Table 3. The pure TiO_2 powder used in this work has a small BET surface area ($10.17\ m^2\ g^{-1}$), which was consistent with a literature value [20]. When ENR_{50}/PVC polymer blend was added to form TiO_2-ENR_{50}-PVC composite, the surface area decreased significantly by almost half of the original value. This is consistent with the results of SEM whereby most of the non-etched immobilized TiO_2-ENR_{50}-PVC surface was covered with the polymer blend. However, compared with pure TiO_2, the surface areas of the photo-etched immobilized TiO_2-ENR_{50}-PVC composite were increased while its pore diameter decreased. These smaller pores possibly account for the larger surface area of the photo-etched immobilized TiO_2 composite. This result amplifies the useful technique of using ENR_{50}/PVC blend as the adhesive for immobilizing the TiO_2 powder onto solid supports such as glass plates since their subsequent etching process enhances the surface properties of the immobilized system.

3.3.1. Photocatalytic Degradation of MB Solution by the Photo-Etched Immobilized TiO_2-ENR_{50}-PVC Composite. As shown in Figure 7, only $10.53 \pm 1.15\%$ of MB was photolysed within

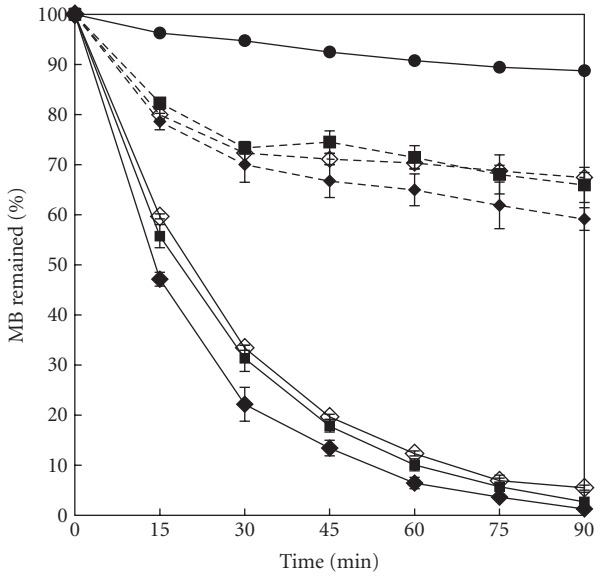

Figure 7: Degradation of MB by photolysis (black circle), TiO_2 powder (black square), non-etched TiO_2-ENR_{50}-PVC (white diamond), and photo-etched TiO_2-ENR_{50}-PVC composite (black diamond) via irradiation under 45 W compact fluorescent lamp with UV leakage of 4.35 Wm^{-2} (continous line) and adsorption in the dark (dashed line).

90 min in the absence of the photocatalyst while the adsorption of MB by the photo-etched TiO_2 composite achieved 35% removal. The photocatalytic degradation of MB by the non-etched immobilized TiO_2 composite achieved 94% removal within 90 minutes of irradiation. However, about 99% of MB was degraded by the photo-etched immobilized TiO_2 composite. In fact, the photocatalytic degradation of MB dye by the photo-etched immobilized TiO_2 composite was found to be better than the TiO_2 powder mode (Figure 7) whereby 97% of the dye was degraded by that system. The pseudo-first-order rate constant calculated from the linear plots based on (2) was 0.047 min^{-1} for the photo-etched TiO_2 composite. This value is slightly higher than 0.040 min^{-1}, which is the pseudo-first-order rate constant produced by the TiO_2 slurry mode. A non-etched TiO_2 composite system produced a pseudo-first-order rate constant of 0.036 min^{-1}. This improved performance of the photo-etched immobilized TiO_2 system was definitely due to the bigger BET surface area achieved during its preparation. As can be seen in Figure 7, the photo-etched photocatalyst system has a better adsorption behavior of MB as compared to the rest of the system. Since photocatalytic degradation of the dye happens principally on the photocatalyst surface, the adsorption of the dye molecules from aqueous solution on TiO_2 surface is very important. This would allow the photogenerated oxidizing radicals to react effectively with the organic pollutants. It is suggested that the reasonably good adsorption capacity of the photo-etched TiO_2 composite can be associated with its bigger surface area.

3.3.2. Reusability and Sustainability of the Photo-Etched Immobilized TiO_2-ENR_{50}-PVC Composite. The reusability and sustainability of the photo-etched immobilized TiO_2-ENR_{50}-PVC composite in the photocatalytic degradation of MB is shown in Figure 8. The photocatalytic efficiency of TiO_2 composite was consistent throughout the 10 subjected cycles whereby more than 98% of the MB was consistently degraded from the first cycle until the tenth cycle of applications. The pseudo-first-order rate constants were also fairly consistent throughout the reuse of the immobilized photocatalyst plate whereby the average pseudo-first-rate constant was $0.054 \pm 0.003\ min^{-1}$. The cleaning-up process of the used photo-etched immobilized TiO_2 system was done by subjecting the photocatalyst plate to 30 min of irradiation with light in ultra pure water after each run in order to clear up the accumulation of MB dye substrates and any intermediates. The photo-etched immobilized TiO_2-ENR_{50}-PVC composite system therefore possesses good sustainability and reusability upon its recycled applications. It was also noted that the fabricated photocatalyst plate was essentially intact after 10 cycles of applications and can certainly be reused for many more applications.

3.3.3. Mineralization of MB by the Photo-Etched Immobilized TiO_2-ENR_{50}-PVC Composite. Preliminary mineralization study of MB solution under photocatalytic treatment by TiO_2 slurry mode and the photoetched immobilized TiO_2 composite was carried out via COD analyses. The kinetics of the COD removal at different reaction times is shown in Figure 9. It was observed that in the course of 8 h of irradiation, the reduction of the COD concentration of 20 mg L^{-1} MB by TiO_2 in the slurry mode achieved 99% as compared to 95% when the photo-etched TiO_2 composite system was used. These values are not far apart which once again proved that immobilization of TiO_2 via this technique did not reduce much of the mineralization efficiency of the photocatalyst system with respect to its slurry counterpart. In fact, Figure 9 shows that COD reduction for photo-etched TiO_2 composite was faster than the slurry system during the first 4 h of irradiation but became slower than the slurry system onwards. This phenomenon can be due to the interference from the formed intermediates that might get adsorbed and accumulate on the fixed surface of the catalyst and reduced the efficiency of the catalyst. It was also observed that the total decolourization of MB in both systems was achieved in less than 4 h, as shown in Supplementary Figure 1. As expected, the decolourization of the dye occurred much faster than the mineralization process since the former process only involved the breakdown of the chromophore while the latter required conversion of all organics into CO_2 and H_2O.

The photomineralization process also yielded anions such as SO_4^{2-}, NO_3^-, and Cl^- as detected by ion chromatography. The result, shown in Figure 10, depicts the concentration of each of the anions found in the treated MB solution. In addition, the solution also became acidic with time indicating the production of H^+ ions, as discussed by Lachheb et al. [21]. The solution pH decreased from pH 7 to 4 after the photocatalytic treatment. As suggested by Fabiyi and Skelton

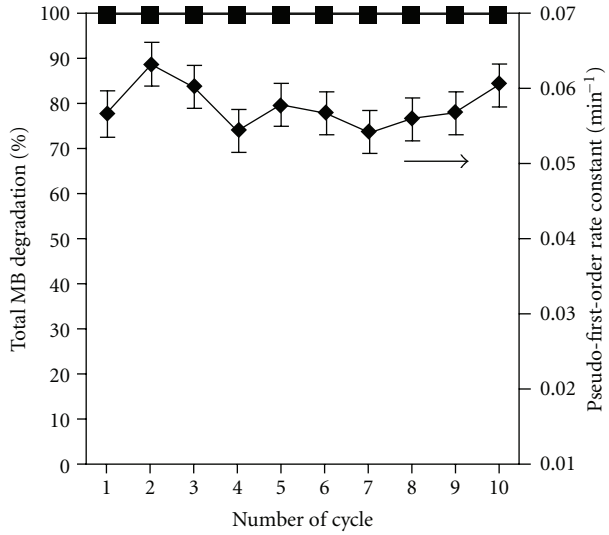

Figure 8: Total percentage of MB solution degradation in each cycle up to 10 cycles of photocatalytic activity over the reused photo-etched TiO_2-ENR_{50}-PVC composite (black square) and their corresponding pseudo-first-order rate constants (black diamond).

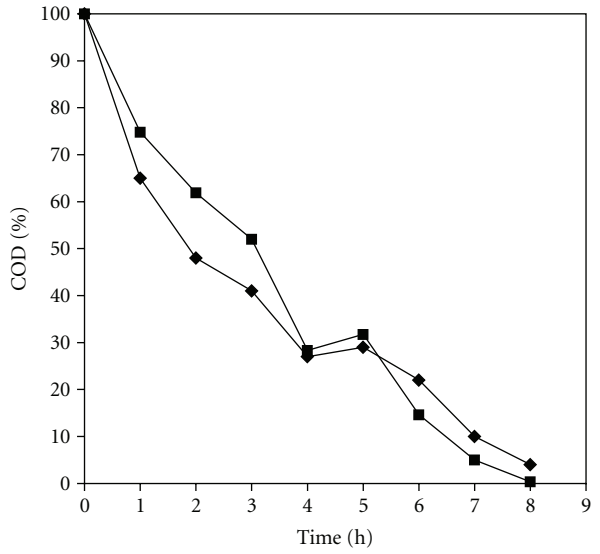

Figure 9: Reduction efficiencies of COD by TiO_2 powder (black square) and photo-etched TiO_2-ENR_{50}-PVC composite (black diamond).

[22] and Lachheb et al., [21], the stoichiometric equation of MB total mineralization is as follows (6):

$$C_{16}H_{18}N_3SCl + 25\frac{1}{2}O_2 \xrightarrow{TiO_2,\ \text{Air},\ h\nu > 3.2\,\text{eV}} 16CO_2 + 6H_2O + 3HNO_3 + H_2SO_4 + HCl \quad (6)$$

The initial step of MB degradation can be ascribed to the attack on the R–S^+=R′ functional group in MB by the photogenerated $OH^\bullet$ radicals, producing sulfonyl or SO_3^-,

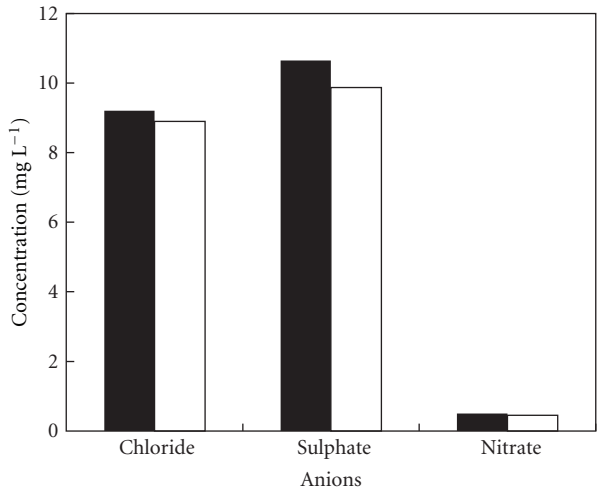

Figure 10: Concentration of anions chloride, sulphate, and nitrate found in MB solution after photocatalytic treatment by photo-etched TiO_2-ENR_{50}-PVC composite (coloured) and TiO_2 in slurry mode (opened).

containing intermediates that lead to the evolution of SO_4^{2-} ions [23]. One possible pathway of this reaction is as presented by the following equations [23]:

$$\begin{aligned} OH^- + h^+ &\longrightarrow OH^\bullet \\ R\text{–}S^+\text{=}R' + OH^\bullet &\longrightarrow R\text{-}S(=O)\text{–}R' + H^+ \\ NH_2\text{–}C_6H_3(R)\text{–}S(=O)\text{–}C_6H_4\text{-}R + OH^\bullet &\longrightarrow NH_2\text{–}C_6H_4\text{–}R + SO_2\text{–}C_6H_4\text{–}R \\ SO_2\text{–}C_6H_4\text{–}R + OH^\bullet &\longrightarrow R\text{–}C_6H_4\text{–}SO_3H \\ R\text{–}C_6H_4\text{–}SO_3H + OH^\bullet &\longrightarrow R\text{–}C_6H_4{}^\bullet + SO_4^{2-} + 2H^+ \end{aligned} \quad (7)$$

Another product of the mineralized MB is NO_3^- ions. The NO_3^- ions are produced by the subsequent oxidization of NH_4^+ ions which are the product of successive attacks by H^+ atoms on nitrogen atoms in MB structure. The oxidation of NH_4^+, leading to the formation of NO_3^- correlates with the stable oxidation of nitrogen (+5) [21]. This formation of NO_3^- is provided by the following equations [21]:

$$\begin{aligned} NH_2\text{–}C_6H_4\text{–}R + H^+ &\longrightarrow C_6H_4\text{–}R^+ + NH_3 \\ NH_3 + 2H_2O + 6\,h^+ &\longrightarrow NO_2^- + 7H^+ \\ NO_2^- + H_2O + 2\,h^+ &\longrightarrow NO_3^- + 2H^+ \end{aligned} \quad (8)$$

The carbonaceous components of the intermediates were then continued to be mineralized eventually into CO_2 and H_2O.

4. Conclusion

The paper showed that a reusable photo-etched immobilized TiO_2-ENR_{50}-PVC composite that possessed slightly better

photocatalytic efficiency than the TiO_2 slurry mode can be successfully prepared via a simple dip-coating method. This low cost but effective method utilized a dip-coating emulsion prepared by mixing TiO_2 powder with ENR_{50}/PVC in mixed solvent system via ultrasonication before being immobilized on glass plates. Photodegradability of ENR_{50}/PVC within the TiO_2 composite under the irradiation of the applied light source (45 W compact fluorescent lamp) allowed us to etch out the polymer blend thus enhanced the surface properties of the system. It was observed that this technique produced a slightly bigger surface area than the initial TiO_2 powder. The photo-etched immobilized TiO_2-ENR_{50}-PVC composite performed at par or better than the TiO_2 slurry mode system. It was highly reusable with sustainable photocatalytic efficiencies in the photocatalytic degradation of MB solution. The photomineralization capability of the photo-etched TiO_2-ENR_{50}-PVC composite was also comparable to the TiO_2 slurry mode system. Therefore, it can be said that the photo-etching technique is a potential new approach in fabricating immobilized TiO_2 system without facing the usual reduction in photocatalytic activity as commonly observed for immobilized photocatalyst systems. Such efficient immobilized photocatalyst system offers excellent advantage of use and reuse without the need to filter the treated water after the treatment and can be easily adapted for continuous flow reactor.

Acknowledgments

The authors thank Ministry of Science and Technology (MOSTI) of Malaysia and Universiti Sains Malaysia (USM) for their generous financial assistance under Grant FRGS: 203/227/PKIMIA/67/027 and IRPA: 305/229/PKIMIA/613402. The authors are also grateful to the Institute of Postgraduate Studies (IPS) USM for Fellowship Scheme and the facilities provided by the USM throughout this research.

References

[1] O. Prieto, J. Fermoso, Y. Nuñez, J. L. Del Valle, and R. Irusta, "Decolouration of textile dyes in wastewaters by photocatalysis with TiO_2," *Solar Energy*, vol. 79, no. 4, pp. 376–383, 2005.

[2] M. Saquib, M. Abu Tariq, M. Faisal, and M. Muneer, "Photocatalytic degradation of two selected dye derivatives in aqueous suspensions of titanium dioxide," *Desalination*, vol. 219, no. 1–3, pp. 301–311, 2008.

[3] R. Jain and M. Shrivastava, "Photocatalytic removal of hazardous dye cyanosine from industrial waste using titanium dioxide," *Journal of Hazardous Materials*, vol. 152, no. 1, pp. 216–220, 2008.

[4] C. Guillard, H. Lachheb, A. Houas, M. Ksibi, E. Elaloui, and J. M. Herrmann, "Influence of chemical structure of dyes, of pH and of inorganic salts on their photocatalytic degradation by TiO_2 comparison of the efficiency of powder and supported TiO_2," *Journal of Photochemistry and Photobiology A*, vol. 158, no. 1, pp. 27–36, 2003.

[5] C. M. Ling, A. R. Mohamed, and S. Bhatia, "Performance of photocatalytic reactors using immobilized TiO_2 film for the degradation of phenol and methylene blue dye present in water stream," *Chemosphere*, vol. 57, no. 7, pp. 547–554, 2004.

[6] G. Mascolo, R. Comparelli, M. L. Curri, G. Lovecchio, A. Lopez, and A. Agostiano, "Photocatalytic degradation of methyl red by TiO_2: comparison of the efficiency of immobilized nanoparticles versus conventional suspended catalyst," *Journal of Hazardous Materials*, vol. 142, no. 1-2, pp. 130–137, 2007.

[7] K. V. S. Rao, M. Subrahmanyam, and P. Boule, "Immobilized TiO_2 photocatalyst during long-term use: decrease of its activity," *Applied Catalysis B*, vol. 49, no. 4, pp. 239–249, 2004.

[8] M. Jin, X. Zhang, A. V. Emeline, T. Numata, T. Murakami, and A. Fujishima, "Surface modification of natural rubber by TiO_2 film," *Surface and Coatings Technology*, vol. 202, no. 8, pp. 1364–1370, 2008.

[9] C. Sriwong, S. Wongnawa, and O. Patarapaiboolchai, "Photocatalytic activity of rubber sheet impregnated with TiO_2 particles and its recyclability," *Catalysis Communications*, vol. 9, no. 2, pp. 213–218, 2008.

[10] V. P. Silva, M. P. Paschoalino, M. C. Gonçalves, M. I. Felisberti, W. F. Jardim, and I. V. P. Yoshida, "Silicone rubbers filled with TiO_2: characterization and photocatalytic activity," *Materials Chemistry and Physics*, vol. 113, no. 1, pp. 395–400, 2009.

[11] M. A. Nawi, L. C. Kean, K. Tanaka, and M. S. Jab, "Fabrication of photocatalytic TiO_2-epoxidized natural rubber on Al plate via electrophoretic deposition," *Applied Catalysis B*, vol. 46, no. 1, pp. 165–174, 2003.

[12] M. A. Nawi, A. H. Jawad, S. Sabar, and W. S. W. Ngah, "Immobilized bilayer TiO_2/chitosan system for the removal of phenol under irradiation by a 45 watt compact fluorescent lamp," *Desalination*, vol. 280, no. 1–3, pp. 288–296, 2011.

[13] C. T. Ratnam and K. Zaman, "Stabilization of poly(vinyl chloride)/epoxidized natural rubber (PVC/ENR) blends," *Polymer Degradation and Stability*, vol. 65, no. 1, pp. 99–105, 1999.

[14] U. S. Ishiaku and Z. A. M. Ishak, "Developments in poly (vinyl chloride)/Epoxidized Natural Rubber Blends," in *Polymer Blends and Alloys*, G. O. Shonaike and G. P. Simon, Eds., Marcel Dekker, New York, NY, USA, 1999.

[15] M. C. S. Perera, U. S. Ishiaku, and Z. A. M. Ishak, "Thermal degradation of PVC/NBR and PVC/ENR50 binary blends and PVC/ENR50/NBR ternary blends studied by DMA and solid state NMR," *Polymer Degradation and Stability*, vol. 68, no. 3, pp. 393–402, 2000.

[16] C. T. Ratnam and K. Zaman, "Modification of PVC/ENR blend by electron beam irradiation: effect of crosslinking agents," *Nuclear Instruments and Methods in Physics Research, Section B*, vol. 152, no. 2, pp. 335–342, 1999.

[17] S. Cho and W. Choi, "Solid-phase photocatalytic degradation of PVC-TiO_2 polymer composites," *Journal of Photochemistry and Photobiology A*, vol. 143, no. 2-3, pp. 221–228, 2001.

[18] S. S. Chin, T. M. Lim, K. Chiang, and A. G. Fane, "Factors affecting the performance of a low-pressure submerged membrane photocatalytic reactor," *Chemical Engineering Journal*, vol. 130, no. 1, pp. 53–63, 2007.

[19] M. N. Radhakrishnan Nair, G. V. Thomas, and M. R. Gopinathan Nair, "Thermogravimetric analysis of PVC/ELNR blends," *Polymer Degradation and Stability*, vol. 92, no. 2, pp. 189–196, 2007.

[20] K. Khuanmar, W. Wirojanagud, P. Kajitvichyanukuk, and S. Maensiri, "Photocatalysis of phenolic compounds with synthesized nanoparticles TiO_2/Sn2," *Journal of Applied Sciences*, vol. 7, no. 14, pp. 1968–1972, 2007.

[21] H. Lachheb, E. Puzenat, A. Houas et al., "Photocatalytic degradation of various types of dyes (Alizarin S, Crocein Orange

G, Methyl Red, Congo Red, Methylene Blue) in water by UV-irradiated titania," *Applied Catalysis B*, vol. 39, no. 1, pp. 75–90, 2002.

[22] M. E. Fabiyi and R. L. Skelton, "Photocatalytic mineralisation of methylene blue using buoyant TiO_2-coated polystyrene beads," *Journal of Photochemistry and Photobiology A*, vol. 132, no. 1-2, pp. 121–128, 2000.

[23] A. Houas, H. Lachheb, M. Ksibi, E. Elaloui, C. Guillard, and J. M. Herrmann, "Photocatalytic degradation pathway of methylene blue in water," *Applied Catalysis B*, vol. 31, no. 2, pp. 145–157, 2001.